VŠB- TECHNICAL UNIVERSITY OF OSTRAVA
FACULTY OF MECHANICAL ENGINEERING
DEPARTMENT OF POWER ENGINEERING

Study of the Influence of Intake Air Temperature to Combustion Turbine Efficiency

Studie vlivu teploty nasávaného vzduchu na účinnost spalovací turbíny

Student: Dharma Rooban Moorthi

Supervisor: Ing. Petr Pavlík, Ph.D.

Ostrava 2021

VŠB - Technical University of Ostrava
Faculty of Mechanical Engineering
Department of Power Engineering

Diploma Thesis Assignment

Student: **Dharma Rooban Moorthi**

Study Programme: N2301 Mechanical Engineering

Study Branch: 2302T006 Energy Engineering

Title: Study of the Influence of Intake Air Temperature to Combustion Turbine Efficiency
Studie vlivu teploty nasávaného vzduchu na účinnost spalovací turbíny

The thesis language: English

Description:

Create a study of the influence of intake air temperature on the efficiency of the SR-30 microturbine learning model. Also process a correlation analysis of the device's efficiency on the intake air temperature.

Content of the diploma thesis:
1. Background research in the field of combustion turbines for mobile and stationary applications.
2. Design of suction pipe flange for installation of air heater.
3. Design drawing of the proposed suction pipe flange.
4. Calculation of the efficiency of the device depending on the intake air temperature, considering isentropic efficiency of the turbine driving a generator ηisoTUR2=86%.
5. Correlation analysis of device efficiency on intake air temperature.

References:

BATHIE, William W. Fundamentals of gas turbines. New York: Wiley, c1984. ISBN 0-471-86285-1.
GIAMPAOLO, Tony. Gas turbine handbook: principles and practice. 5th ed. Lilburn: Fairmont Press ; Boca Raton, c2014. ISBN 978-0-88173-712-7.
TREAGER, Irwin E. Aircraft gas turbine engine technology. 3rd ed. Boston: McGraw-Hill Higher Education, c1996. ISBN 0-02-801828-1.
CHAVKIN, Jurij I. Combustion system design. Tulsa: PennWell Books, c1996. ISBN 0-87814-462-5.
WINTERBONE, D. E. Advanced thermodynamics for engineers. New York: J. Wiley, c1997. ISBN 034067699X.
HORLOCK, J. H. Advanced gas turbine cycles. Malbar, FL: Krieger Pub, 2007. ISBN 1575242923.

Extent and terms of a thesis are specified in directions for its elaboration that are opened to the public on the web sites of the faculty.

Supervisor: **Ing. Petr Pavlík, Ph.D.**

Date of issue: 18.12.2020
Date of submission: 17.05.2021

doc. Ing. Stanislav Honus, Ph.D.
Head of Department

prof. Ing. Robert Čep, Ph.D.
Dean

Student's affidavit

I declare that I have prepared the whole diploma thesis including appendices independently under the leadership of the diploma thesis supervisor, and I stated all the documents and literature used.

In Ostrava on May 17, 2021.

Student's Signature

I declare that:

- I am aware that Act No. 121/2000 Coll., Act on copyright, rights related to copyright and amending some laws (the Copyright Act), in particular Section 35 (Use of a work in the civil or religious ceremonies or in official events organized by public authorities, in the context of university performance and use of university work) and Section 60 (university work) shall apply to my Diploma thesis
- I understand that VŠB – Technical University of Ostrava (hereinafter referred to as "VŠB-TUO") has the right to use this final Diploma thesis non- commercially for its internal use (Section 35 Subsection 3 of the Copyright Act)
- If requested, a copy of this Diploma thesis will be deposited with the thesis supervisor,
- If VŠB-TUO is interested, I will make a licensing agreement with it permitting to use the thesis within the scope of Section 12 Subsection 4 of the Copyright Act,
- I can only use my thesis, or grant a license to use it with the consent of VŠB- TUO, which is authorized in such a case to demand an appropriate contribution to the costs that were incurred by VŠB-TUO to create the thesis (up to the actual amount),
- I understand that - according to Act No.111/1998 Coll., on higher education institutions and on changes and amendments to other acts (Higher Education Act), as amended - that this Diploma thesis will be available for public before the defense at the thesis supervisor's workplace, and electronically stored and published after the defense at the Central Library of VŠB-TUO, regardless of the outcome of its defense.

In Ostrava on May 17, 2021

Signature of the author

Name and surname of the thesis author: Dharma Rooban Moorthi

Permanent address of the thesis author: 5/312, Gokula Nagar, Kumbaram, Ramanathapuram – 623523. Tamil Nadu, India.

ANNOTATION

Dharma Rooban Moorthi. Information System Creation: Diploma Thesis. Ostrava: VŠB-Technical University of Ostrava, Faculty of Mechanical Engineering, Department of Power Engineering, 2021. Thesis head: Ing. Petr Pavlik, Ph.D.

This diploma thesis dealing with the study of the influence of intake air temperature on the efficiency of the SR-30 microturbine learning model. Also, process a correlation analysis of the device's efficiency on the intake air temperature.

ANOTACE

Dharma Rooban Moorthi. Tvorba informačního systému: Diplomová práce. Ostrava: VŠB-Technická univerzita Ostrava, Fakulta strojního inženýrství, Katedra energetiky, 2021. Vedoucí DP: Ing. Petr Pavlik, Ph.D.

Tato diplomová práce se zabývá studiem vlivu teploty nasávaného vzduchu na účinnost modelu učení mikroturbíny SR-30.Také proveďte korelační analýzu účinnosti zařízení s teplotou nasávaného vzduchu.

Table of Content:

List of Figures:

List of Tables:

Nomenclature:

a_K	Compressor work	*kJ/Kg*
a_T	Turbine work	*kJ/kg*
a_{Kie}	Ideal compressor work	*kJ/kg*
a_{Tie}	Ideal turbine work	*kJ/kg*
a_0	Work done	*kJ/kg*
m_{vz}	Amount of inlet air	$kg.s^{-1}$
m_p	Fuel flow	*l/h*
N	Speed	*rpm*
P	Pressure of the compressor, turbine, nozzle	*kPa*
PSF	Profile shape factor	-
PT	Power extraction turbine	-
P_k	Compressor power	*kW*
P_T	Turbine power	*kW*
s_K	Suction flow cross section	m^2
T	Temperature of the compressor, turbine, nozzle	°*C*
T_{ex}	Exhaust gas temperature	°*C*
VA	Volumetric fuel flow rate	*cc/min*
w_{vz}	Intake air speed	$m.s^{-1}$
η	Efficiency	-
η_c	Compressor adiabatic efficiency	-
η_T	Turbine adiabatic efficiency	-
η_N	Exhaust nozzle efficiency	-
η_{kie}	Thermodynamic compressor efficiency	%
η_{Tie}	Thermodynamic turbine efficiency	%
η_{total}	Overall device efficiency	%
ρ	Fuel density	kg/m^3
ρ_{vz}	Constant air density	kg/m^3
1….6	Relation of compressor, turbine, nozzle inlet and outlet of temperature and pressure difference	-
ex	Compressor, turbine exit	-
in	Compressor, turbine inlet	-
Δi, $i_{1\ldots4}$	Enthalpy difference	*kJ/kgK*

K	Compressor	-
T	Turbine	-

1 Introduction

The main objective of this project is to study of the influence of intake air temperature on the efficiency of the SR-30 microturbine learning model. Also process a correlation analysis of the device's efficiency on the intake air temperature. The current study investigated about combustion turbine efficiency by calculating intake air at different temperature. This project described about the working process of SR-30 microturbine and performance characteristics analysis of intake air temperature.

By using Data acquisition software, we measure Gas Turbine Run Data in preparation for system analysis and performance calculations. Personal Daq data acquisition systems directly measure multiple channels of voltage, thermocouples, pulse, frequency, and digital I/O. The main motivation of our project is to increase the combustion turbine efficiency.

The gas turbines are one of the most widely-used power generating technologies. Gas turbines are a type of internal combustion (IC) engine in which burning of an air-fuel mixture produces hot gases that spin a turbine to produce power. It is the production of hot gas during fuel combustion, not the fuel itself that the gives gas turbines the name[1]. Gas turbines can utilize a variety of fuels, including natural gas, fuel oils, and synthetic fuels. Combustion occurs continuously in gas turbines, as opposed to reciprocating IC engines, in which combustion occurs intermittently[1].

The SR-30 is a small-scale, turbojet engine which sounds and smells like a real engine used to fly commercial aircraft. With an overall length of less than 2.0 feet and an average diameter of 6.5 inches, the SR-30 is equipped with an inlet nozzle, radial compressor, counter-flow combustion chamber, turbine, and exhaust nozzle[2]. Although it can operate on various fuels, diesel fuel is used in the studies described here, and each component is instrumented with thermocouples and pressure gages to allow a complete thermodynamic evaluation. Screaming along at 80,000 *rpm* and sending out exhaust gas at 500 mph, the SR-30 engine is fun science for students! However, since the SR-30 was essentially designed for one-dimensional measurement and flow analysis, students quickly learn the limitations of these assumptions[2].

By considering the problems of the world about the supply of fuel, the high cost of energy transfer and also the movement of reduction of underground fuel reserves, any slight increase in the power generation's efficiency will cause a significant reduction in fuel assumption and cost saving in generation[3]. The basic operation of the gas turbine is similar to that of the steam power plant except that air is used instead of water. Fresh atmospheric air flows

through a compressor that brings it to higher pressure. Energy is then added by spraying fuel into the air and igniting it so the combustion generates a high temperature flow. This high-temperature high-pressure gas enters a turbine, where it expands down to the exhaust pressure, producing a shaft work output in the process. The turbine shaft work is used to drive the compressor and other devices such as an electric generator that may be coupled to the shaft[3]. The energy that is not used for shaft work comes out in the exhaust gases, so these have either a high temperature or a high velocity. The purpose of the gas turbine determines the design so that the most desirable energy form is maximized. Gas turbines are used to power aircraft, trains, ships, electrical generators, or even tanks[3].

One of the main methods used to increase the gas turbine efficiency is the heating of the compressor intake air. Gas turbine performance is critically limited by the amounting ambient temperature, mainly in hot and dry regions[3]. It occurs because the power output is inversely proportional to the ambient temperature. In the current study, the effect of intake air temperature is studied and gas thermal efficiency are also obtained. The gas turbine efficiency is also tested with different climate conditions[3].

2 Combustion Gas Turbine

Gas turbine engines derive their power from burning fuel in a combustion chamber and using the fast-flowing combustion gases to drive a turbine in much the same way as the high-pressure steam drives a steam turbine[4]. A simple gas turbine is comprised of three main sections: a compressor, a combustor, and a power turbine. The gas turbine operates on the principle of the Brayton cycle, where compressed air is mixed with fuel and burned under constant pressure conditions. The resulting hot gas is allowed to expand through a turbine to perform work[4].

2.1 Working Principle

Gas turbines are comprised of three primary sections mounted on the same shaft: the compressor, the combustion chamber (or combustor) and the turbine. The compressor can be either axial flow or centrifugal flow[1]. Axial flow compressors are more common in power generation because they have higher flow rates and efficiencies. Axial flow compressors are comprised of multiple stages of rotating and stationary blades (or stators) through which air is drawn in parallel to the axis of rotation and incrementally compressed as it passes through each stage. The acceleration of the air through the rotating blades and diffusion by the stators increases the pressure and reduces the volume of the air. Although no heat is added, the compression of the air also causes the temperature to increase[1].

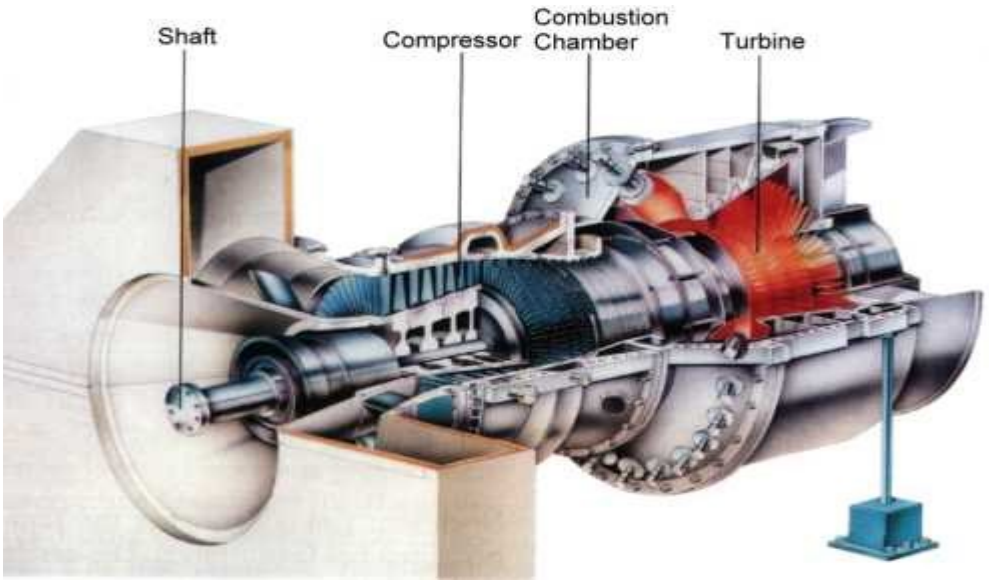

Figure 2.1 Combustion Turbine

Source: https://www.wartsila.com/energy/learn-more/technical-comparisons/gas-turbine-for-power-generation-introduction

The compressed air is mixed with fuel injected through nozzles. The fuel and compressed air can be pre-mixed or the compressed air can be introduced directly into the combustor. The fuel-air mixture ignites under constant pressure conditions and the hot combustion products (gases) are directed through the turbine where it expands rapidly and imparts rotation to the shaft. The turbine is also comprised of stages, each with a row of stationary blades (or nozzles) to direct the expanding gases followed by a row of moving blades[1]. The rotation of the shaft drives the compressor to draw in and compress more air to sustain continuous combustion. The remaining shaft power is used to drive a generator which produces electricity. Approximately 55 to 65 percent of the power produced by the turbine is used to drive the compressor. To optimize the transfer of kinetic energy from the combustion gases to shaft rotation, gas turbines can have multiple compressor and turbine stages[1].

Because the compressor must reach a certain speed before the combustion process is continuous – or self-sustaining – initial momentum is imparted to the turbine rotor from an external motor, static frequency converter, or the generator itself. The compressor must be smoothly accelerated and reach firing speed before fuel can be introduced and ignition can occur[1]. Turbine speeds vary widely by manufacturer and design, ranging from 2,000 revolutions per minute *rpm* to 10,000 *rpm*. Initial ignition occurs from one or more spark plugs (depending on combustor design). Once the turbine reaches self-sustaining speed – above 50% of full speed – the power output is enough to drive the compressor, combustion is continuous, and the starter system can be disengaged[1].

2.2 Theory of Operation

According to the gas turbine theory, the work of this equipment is to convert fuels such as natural gas to mechanical energy. This energy drives a generator for the production of electrical power. It all starts with the ambient air entering the compressor. The compressor increases the temperature and pressure of the air, before directing the transformed air to the combustion chamber[5]. Here, the air-fuel mixture is heated at elevated pressures and temperatures to create an extremely hot gas. This gas goes through the turbine blades accelerating them to an incredibly fast rotation. In other words, it creates work that makes the drive shaft to spin furiously. This process produces electricity that can be fed to the grid. This is what is called an open Brayton Thermodynamic Cycle[5].

In an ideal gas turbine, gases undergo four thermodynamic processes: an isentropic compression, an isobaric (constant pressure) combustion, an isentropic expansion and heat rejection. Together, these make up the Brayton cycle[6].

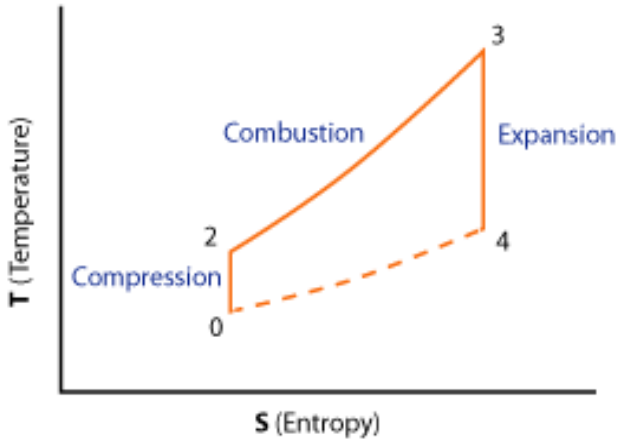

Figure 2.2 Brayton Cycle.

Source:https://en.wikibooks.org/wiki/Jet_Propulsion/Thermodynamic_Cycles/Brayton_cycle

In a real gas turbine, mechanical energy is changed irreversibly (due to internal friction and turbulence) into pressure and thermal energy when the gas is compressed (in either a centrifugal or axial compressor)[6]. Heat is added in the combustion chamber and the specific volume of the gas increases, accompanied by a slight loss in pressure. During expansion through the stator and rotor passages in the turbine, irreversible energy transformation once again occurs. Fresh air is taken in, in place of the heat rejection[6].

3 SR-30 Combustion Gas Turbine

Mini Lab is a self-contained turbojet engine test cell[7]. Utilized by hundreds of leading educational institutions, the included SR30 turbojet engine offers exciting teaching opportunities in applied thermodynamics and jet propulsion[7].

Figure 3.1 Gas Turbine Setup

Source: https://www.turbinetechnologies.com/educational-lab-products/turbojet-engine-lab

A National Instruments based data acquisition system displays and records compressor inlet temperature and pressure, turbine inlet temperature and pressure, turbine exit temperature and pressure, thrust and fuel flow and makes possible studies of[7]:

- Brayton Cycle
- Compressor Performance
- Turbine Performance - work & power, expansion ratio, turbine efficiency
- Combustion/Emissions Analysis

Figure 3.2 SR30 Turbojet Engine

Source: https://www.turbinetechnologies.com/educational-lab-products/turbojet-engine-lab

All engine support systems are fully integrated. The system is easily rolled to any convenient location[7]. No dedicated test cell or facilities modifications are required. The time between delivery and first run is measured in minutes. The included data acquisition system makes real-time engine data display and recording effortless. CAD Models of all primary engine components are also available, along with their flow-cavity negatives, to support CFD or other turbomachinery related analysis[7].

Equipped with the OneTouc Auto Start System, virtually anyone can operate the Mini Lab. Start sequencing is completely automatic with all critical engine parameters monitored during operation. In the unlikely event of an engine fault, the OneTouch system will stop the engine and alert the operator to the problem[7].

The pre-installed Mini Lab Interactive Virtual Instrument Panel displays and records pertinent engine data for follow-on study[7]. This Lab View generated offers a real-time graphical perspective of engine performance. All engine operating parameters are displayed clearly on the engine cutaway graphic[7].

Engine pressures, temperatures and fuel flow are displayed in digital data windows. Engine RPM and thrust are displayed on analog-style round meters for a neat visual cue (the readings are also displayed digitally below each meter) [7].

The real-time plotting feature lets the operator plot any parameter on screen as it occurs to provide a clear sense of how the data is reacting to the actual system operating conditions. Operators can toggle between all the parameters to watch them graphically[7]. Data logging functionality is conveniently controlled from the screen. All the jet engine power data can be observed and tracked through its full throttle range. System units can be changed with a simple click of the mouse. Feeding this interactive is data from the on-board National Instruments 6218 Data Acquisition System. That same data is also stored for later retrieval and analysis and the code is even open for user programming and customization[7]!

The model SR-30 engine is now available in cut-away form. Your students will be able to follow a detailed flow path- from compressor inlet to thrust nozzle exit! The rotating assembly is mounted on ball bearings, which allows for clear and tactile demonstration of rotating and stationary component interaction[8].

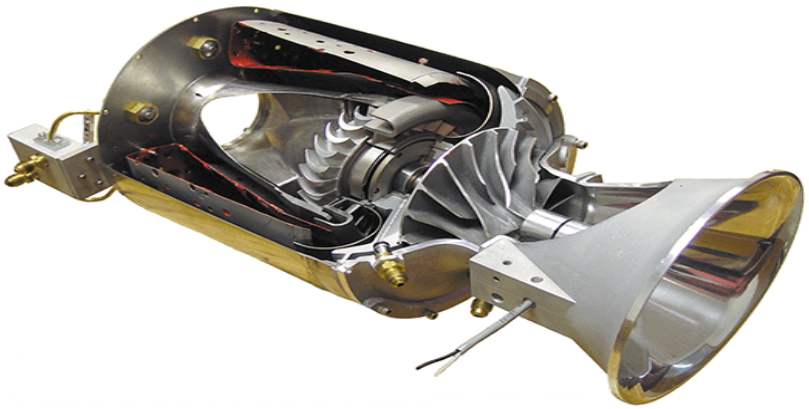

Figure 3.3 SR30 Turbojet Engine Cutaway Model

Source: https://www.turbinetechnologies.com/educational-lab-products/turbojet-engine-lab

The SR-30 is comprised of an axial flow turbine stage consisting of a super alloy cast nozzle vane guide ring and a high nickel content bladed disk turbine wheel[8]. It features a reverse flow annular combustion chamber and 6 high-pressure, return flow fuel atomizer nozzles. Detailed views of bearing components (including oil galley ways), rotating and stationary parts and combustion chamber geometry are also made clearly visible. The ATA approved

flight case is lightweight yet extremely durable. This cut-away engine is designed to carry from classroom to classroom for years to come[8].

3.1 Gas Turbine Cycle

This Gas turbine engine operates on a Brayton cycle. The Brayton cycle depicts the air-standard model of a gas turbine power cycle[9]. A simple gas turbine is comprised of three main components: a compressor, a combustor, and a turbine. According to the principle of the Brayton cycle, air is compressed in the compressor. The air is then mixed with fuel, and burned under constant pressure conditions in the combustor. The resulting hot gas is allowed to expand through a turbine to perform work. Most of the work produced in the turbine is used to run the compressor and the rest is available to run auxiliary equipment and produce power[9].

The gas turbine is used in a wide range of applications. Common uses include stationary power generation plants (electric utilities) and mobile power generation engines (ships and aircraft). In power plant applications, the power output of the turbine is used to provide shaft power to drive a generator, a helicopter rotor, etc. A jet engine powered aircraft is propelled by the reaction thrust of the exiting gas stream[9]. The turbine provides just enough power to drive the compressor and produce the auxiliary power. The gas stream acquires more energy in the cycle than is needed to drive the compressor. The remaining available energy is used to propel the aircraft forward[9].

Shown below in Figure 3.4. is a schematic of the Brayton cycle[9]. Low-pressure air is drawn into a compressor (state 1) where it is compressed to a higher pressure (state 2). Fuel is added to the compressed air and the mixture is burnt in a combustion chamber. The resulting hot gases enter the turbine (state 3) and expand to state 4[9].

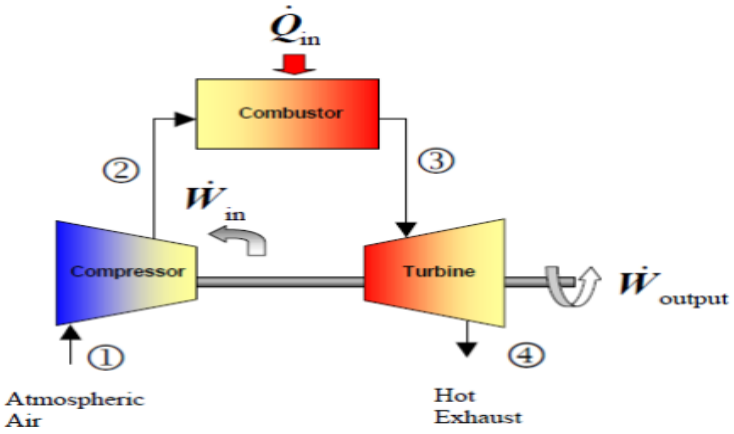

Figure 3.4 Basic Brayton Cycle

Source:https://www.turbinetechnologies.com/Portals/0/pdfs/Wentworth%20Inst%20Tech%20Final_Report_Mini_Jet_Turbine_Analysis_and_Testing.pdf

An analysis on this engine provides important performance characteristics such as thrust, compressor performance, turbine performance (work and power, expansion ratio, turbine efficiency), combustion/emission analysis, and overall isentropic efficiency[9]. In order to perform an analysis on this engine, several quantities at specific locations are needed. Sensors are instrumented on this engine at the compressor inlet, compressor outlet, turbine inlet, turbine exit, and exhaust to collect data on the temperature and pressure at each location. This data is then used to perform a performance analysis on the engine. In addition, there are sensors on this engine to monitor thrust, rpm, and fuel flow rate. Shown below in Figure 3.5. is a cross section of the engine with main components labeled. Figure 3.6. shows the location of each temperature and pressure being measured on the engine[9].

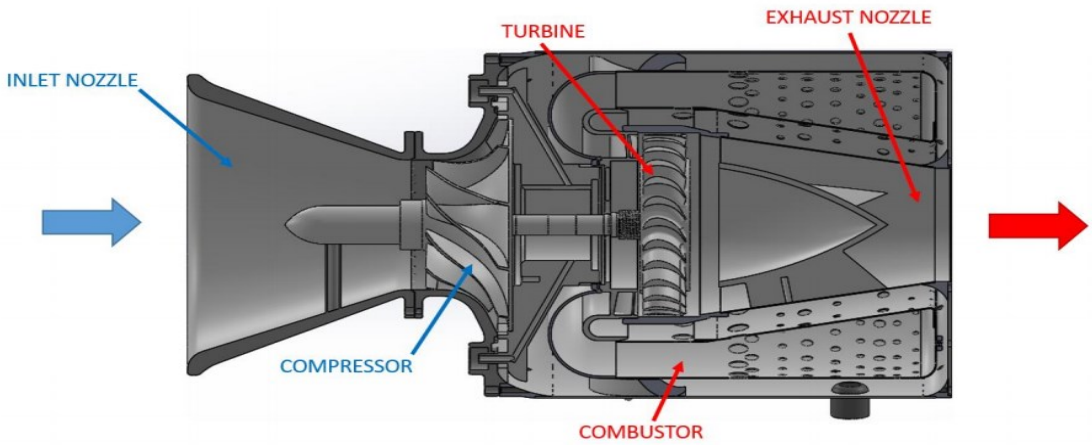

Figure 3.5 Turbine Engine Layout (Brayton Cycle)

Source:https://www.turbinetechnologies.com/Portals/0/pdfs/Wentworth%20Inst%20Tech%20Final_Report_Mini_Jet_Turbine_Analysis_and_Testing.pdf

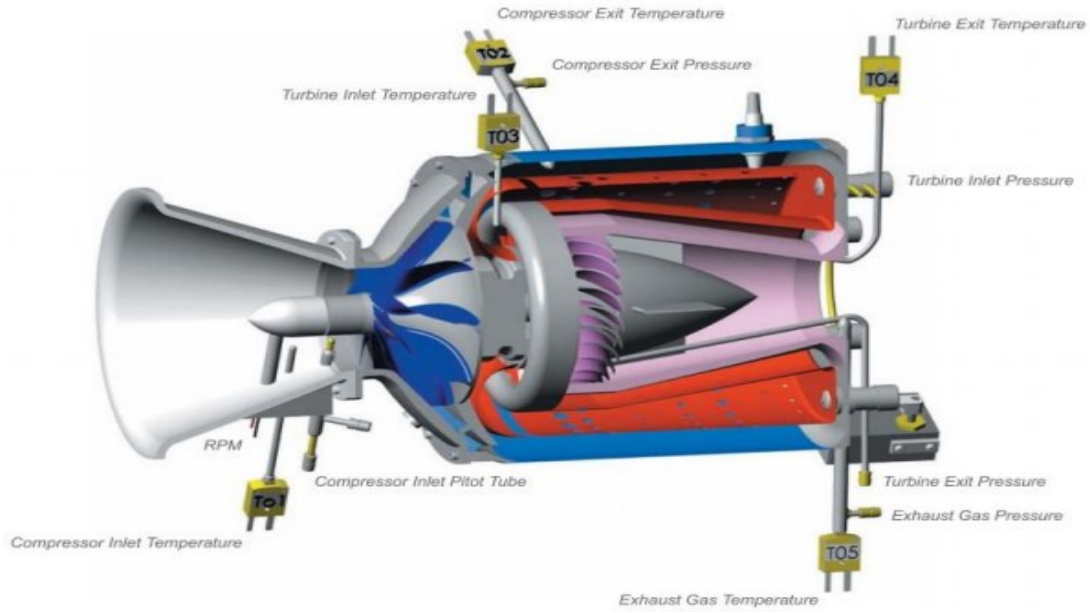

Figure 3.6 Engine Instrumentation Locations

Source:https://www.turbinetechnologies.com/Portals/0/pdfs/Wentworth%20Inst%20Tech%20Final_Report_Mini_Jet_Turbine_Analysis_and_Testing.pdf

3.2 Gas Turbine Controls

In industrial gas turbines, the acceleration rate is limited by the mass moment of inertia of the driven equipment[10]. This responsiveness does not come without a downside. Without a proper control system: the compressor can go into surge in less than 50 milliseconds; the turbine can exceed safe temperatures in less than a quarter of a second; and the power turbine can go into overspeed in less than two seconds. Furthermore, changes in ambient temperature and ambient pressure, deviations that may not even be noticed, can adversely affect the operation of the gas turbine. the gas turbine can take many different forms (single shaft, dual shaft, hot end drive, cold end drive) depending on the application (turbojet, turboprop, generator drive, process compressor drive, process pump drive, etc.). Controlling the gas turbine in each of these different configurations and applications requires the interaction of several complex functions. Some of the complexity can be simplified by considering the gas turbine as a gas generator and a power-extraction-turbine, where the gas generator consists of the compressor, combustor, and compressor turbine[10]. The compressor-turbine is that part of the gas generator developing the shaft horsepower to drive the compressor; and the power-extraction turbine is that part of the gas turbine developing the horsepower to drive the external load. The energy developed in the combustor, by burning fuel under pressure,

is gas horsepower (GHP). On turbojets, the gas horsepower that is not used by the compressor-turbine to drive the compressor is converted to thrust. On turboprops, mechanical drive, and generator drive gas turbines this gas horsepower (designated GHP_{PT}) is used by the power-extraction-turbine to drive the external load. Note that this categorization applies whether the power extraction turbine is a free power turbine or integrally connected to the compressor-turbine shaft. Therefore, whether the gas horsepower is expanded through the remaining turbine stages (as on a single shaft machine), or through a free power turbine (as on a split shaft machine) this additional energy is converted into shaft horsepower (SHP) [10]

This can be represented as follows:

$$\boldsymbol{GHP_{PT=\eta_{PT}SHP}} \qquad \textbf{(0.1)}$$

where η_{PT} = Efficiency of the power extraction turbine.

The control varies SHP of the gas generator turbine and power extraction turbine by varying gas generator speed, which the control accomplishes by varying fuel flow (Figure3.7). Control of the gas turbine in providing the shaft horsepower required by the operation or process is accomplished using parameters such as fuel flow, compressor inlet pressure, compressor discharge pressure, shaft speed, compressor inlet temperatures and turbine inlet or exhaust temperatures[10]. At a constant gas generator speed, as ambient temperature decreases, turbine inlet temperature will decrease slightly and GHP will increase significantly (Figure 2.8). This increase in gas horsepower results from the increase in compressor pressure ratio and aerodynamic loading. Therefore, the control must protect the gas turbine on cold days from overloading the compressor airfoils and over-pressurizing the compressor cases. To get all the power possible on hot days it is necessary to control turbine inlet temperature to constant values, and allow gas generator speed to vary. The control senses ambient inlet temperature, compressor discharge pressure (also referred to as burner pressure-Pb), and gas generator speed[10].

These three variables affect the amount of power that the engine will produce (Figure 2.9). Also, sensing ambient inlet temperature helps ensure that engine internal pressures are not exceeded, and sensing turbine inlet temperature ensures that the maximum allowable turbine temperatures are not exceeded[10]. Sensing gas generator speed enables the control to accelerate through any critical speed points (gas turbines are typically flexible shaft machines and, therefore, have a low critical speed). There are as many variations in controls as there are control manufacturers, gas turbines, and gas turbine applications. Controls can

be divided into several groups: hydromechanical (pneumatic or hydraulic), electrical (hard wired relay logic), and computer (programmable logic controller or microprocessor). The hydromechanical type controls consist of cams, servos, speed (fly-ball) governors, sleeve and pilot valves, metering valves, temperature sensing bellows, etc.[10]

Electrical type controls consist of electrical amplifiers, relays, switches, solenoids, timers, tachometers, converters, thermocouples, etc. Computer controls incorporate many of the electrical functions such as amplifiers, relays, switches, and timers within the central processing unit (CPU). These functions are easily programmed in the CPU and they can be just as easily reprogrammed[10]. This flexibility in modifying all or part of a program is especially useful to the user/operator in the field. Analog signals such as temperature, pressure, vibration, and speed are converted to digital signals before they are processed by the CPU. Also, the output signals to the fuel valve, variable geometry actuator, bleed valve, anti-icing valve, etc. must be converted from digital to analog[10].

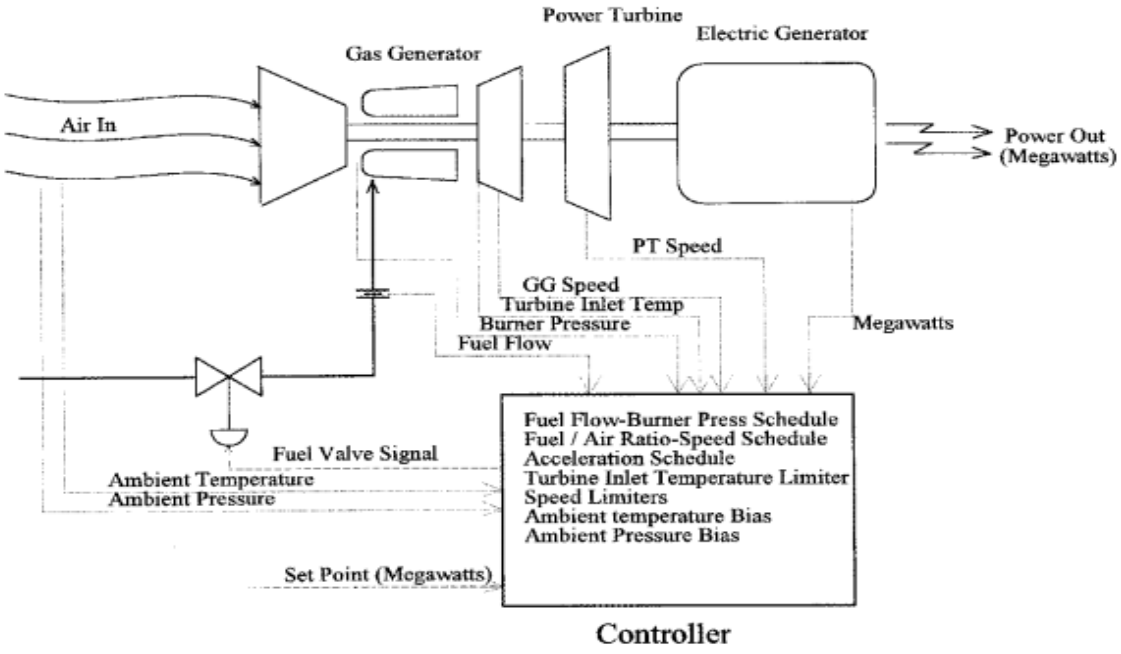

Figure 3.7 Simplified gas turbine-generator control system.

Source: http://payamavad.com/Uploads/Attachements/cf2e31bf-3553-422d-becb-4ec1d49fc06a.pdf

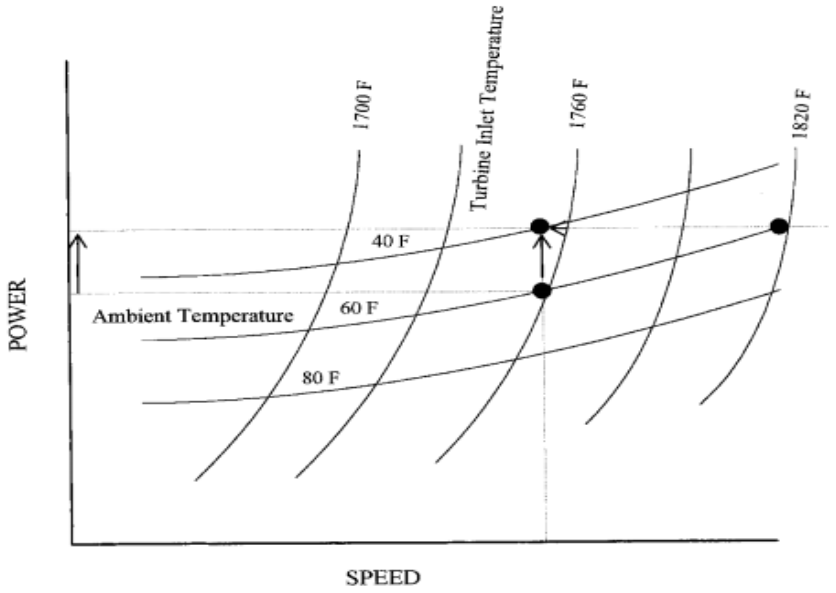

Figure 3.8 Temperature-power-speed interrelationships.

Source: http://payamavad.com/Uploads/Attachements/cf2e31bf-3553-422d-becb-4ec1d49fc06a.pdf

From the turn of the century through the late 1970s, control systems operated only in real time with no ability to store or retrieve data. Hydromechanical controls had to be calibrated frequently (weekly in some applications) and were subject to contamination and deterioration due to wear[10]. A requirement for multiple outputs (i.e., fuel flow control and compressor bleed-air flow-control) required completely independent control loops. Coordinating the output of multiple loops, through cascade control, was a difficult task and often resulted in a compromise between accuracy and response time. In addition, many of the tasks had to be performed manually. For example, station valves, pre lube pumps, and cooling water pumps were manually placed into the running position prior to starting the gas generator. Also, protection devices were limited. The margin between temperature control set points and safe operating turbine temperatures was necessarily large because the hydromechanical controls could not react quick enough to limit high turbine temperatures, or to shut down the gas generator, before damage would occur[10].

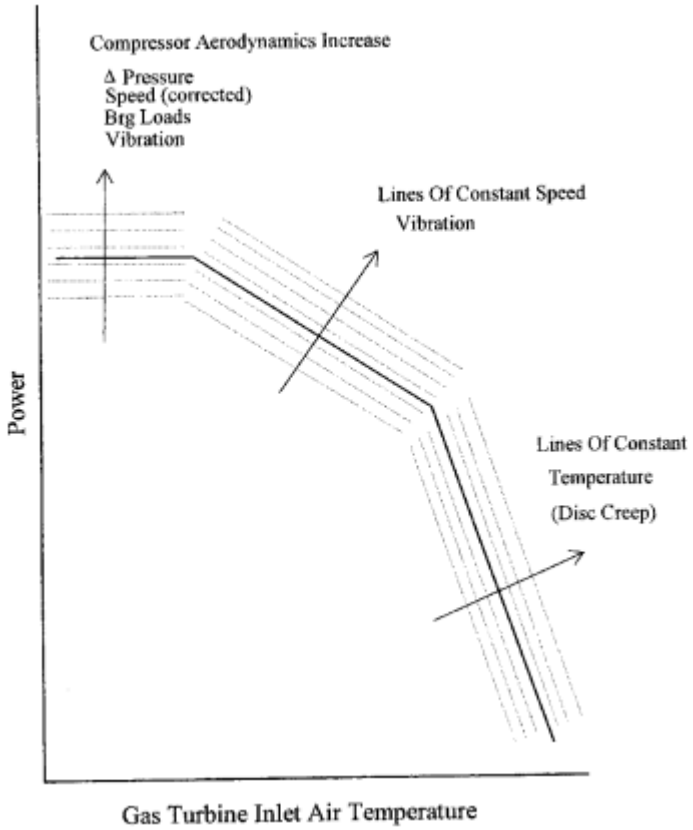

Figure 3.9 Shaft horsepower vs. inlet temperature.

Source: http://payamavad.com/Uploads/Attachements/cf2e31bf-3553-422d-becb-4ec1d49fc06a.pdf

Controls for a typical gas turbine generator or mechanical drive application in the early 1970s were electric controls and consisted of Station Control, a Process Control, and a Turbine Control[10]. In this type of control system all control functions (Start, Stop, Load, Unload, Speed, and Temperature) were generated, biased, and computed electrically. Output amplifiers were used to drive servo valves, employing high pressure hydraulics, to operate hydraulic actuators. These actuators were sometimes fitted with position sensors to provide electronic feedback[10].

4 Engine Components

4.1 Intake Nozzle

Air flow enters the engine through a contoured nozzle prior to contact with the radial compressor. Within the nozzle, at a location where the cross-sectional area is 38.5 cm^2, are placed a thermocouple probe (T_1) $°C$ and pitot-static probe[11]. You will record T1 and Δp1 to compute the ideal intake airflow rate. You will compute the ideal airflow *kg/sec* assuming that the velocity profile at the measurement location is uniform across the nozzle cross section. The actual air flow rate can be measured by taking the difference between the exhaust mass flow (integrated as described below) and the fuel flow rate (through a calibration as described below). From this information we develop a Profile Shape Factor (PSF) for the inlet flow defined as:

$$PSF = m\ air,\ actual\ /\ m\ air,\ based\ on\ centerline^{[11]} \quad \textbf{(0.1)}$$

4.2 Fuel Flow

Fuel flow rates are obtained by measuring the pressure at the fuel injector manifold[11]. The relationship between volumetric fuel flow rate and manifold pressure is given by:

$$(VA)fuel = 4.07\ P\ manifold - 0.013\ P\ manifold\ 2 - 3.7 \quad \textbf{(0.2)}$$

where P is the manifold pressure measured in bar and (VA)fuel is the fuel volumetric flow rate *cc/min*. This equation was obtained by weighing the fuel tank prior to and after test runs of 30 minutes duration, errors in fuel flow can be attributed entirely to the precision error in P manifold. The engine runs on diesel fuel having the following properties:

- 2LHV = 44,470 *kJ/kg*
- Specific gravity = 0.85 (at room temperature and pressure) [11]

4.3 Radial Compressor

Air leaving the intake nozzle enters a radial compressor. Conditions exiting the compressor are measured at (T_2) $°C$ and (P_2) bar. Compressor assumptions will include:

- Steady state operation
- Adiabatic
- Negligible changes in kinetic and potential energy

Following key components should be analyzed:

- Compute the compressor input power requirements (*KW*)
- Compute the compressor adiabatic efficiency, η_c
- Show the ideal and actual compressor states on a T-s diagram[11].

4.4 Combustor

Air leaving the compressor enters a counterflowing combustion chamber[11].Post combustion gases are measured at (T_3) °*C* and (P_3) bar. Combustor assumptions include:

- Steady state operation
- No stray heat loss
- Negligible changes in kinetic and potential energy
- Assume that the post-combustion gases have the properties of air

Important things to be considered in the combustor analysis:

- Compute the actual heat released by the fuel (*KW*)
- Compute the ideal heat released by the fuel (*KW*)
- Compute the combustor efficiency, η_{comb}[11]

4.5 Turbine

Air leaving the turbine enters a nozzle guide vane and then an axial turbine. Conditions downstream of the turbine are measured at (T_4) °*C* and (P_4) bar[11]. Compressor assumptions will include:

- Steady state operation
- Adiabatic
- Negligible changes in kinetic and potential energy

With an emphasis on the following aspects:

- Compute the turbine output power delivered *KW*
- Evaluate the matching requirement, turbine power = compressor power
- Compute the turbine adiabatic efficiency, η_T.
- Show the ideal and actual turbine states on a T-s diagram[11].

4.6 Exhaust flow

The exhaust gases exit the engine through a converging nozzle, where we can make the following assumptions:

- Steady state operation
- Adiabatic
- Negligible changes in potential energy
- Negligible kinetic energy at nozzle inlet (state 4).

Like most real engines, the exhaust flow of the SR-30 is not well behaved. There are considerable variations in temperature and velocity across the nozzle exit plane requiring us to integrate the exhaust flow to get reasonable closure on the engine performance[11]. To accomplish this integration, we will measure an exhaust profile of (T_6) °*C* and (P_6) (dynamic pressure, torr Note: the static pressure at the nozzle exhaust is atmospheric pressure). Measurements will extend across a vertical profile covering the full 54 mm of exhaust nozzle exit diameter. The data sheet provided indicates the locations where the data should be obtained. The following quantities should be derived or provided using the exhaust profile data[11]:

- Plot the exhaust Temperature Profile (Celsius)
- Plot the exhaust Velocity Profile (*m/sec*)
- Integrate the data to obtain the exhaust mass flow rate (*kg/sec*)
- Integrate the data to obtain the engine thrust (Newtons)
- Integrate the data to obtain the kinetic energy of the exhaust gases (*kW*) [11]

From the integrated data, the following quantities can be computed:

- Actual engine air flow rate (*kg/sec*)
- Engine air-fuel ratio
- Intake profile shape factor, PSF
- Exhaust nozzle efficiency,

$$\eta_N = KE \text{ integrated} / KE \text{ ideal} \quad (0.3)$$

4.7 Hush kit

The Hush Kit Gas Turbine Sound Suppressor System is an optional silencer assembly available for installation in the Minilab Gas Turbine Power System[12].Designed to reduce

the sound level of the SR-30 Gas Turbine Engine, the Hush Kit is effective in both the academic and research setting and capable of retrofit to existing installations[12].

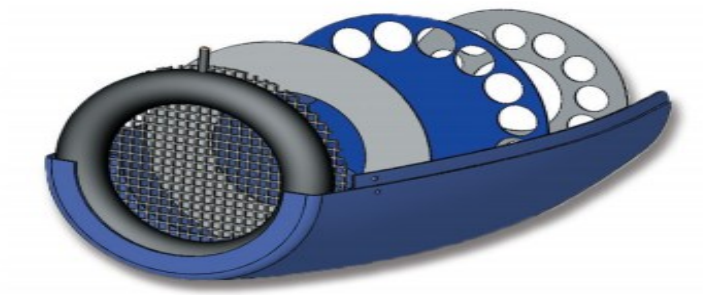

Figure 4.1 Hush kit Internal Design

Source:https://www.turbinetechnologies.com/Portals/0/pdfs/specifications/HushKit%20Specs.pdf

The Hush Kit system is composed of individual intake and exhaust suppressor units[12]. The aircraft style nacelle shaped intake suppressor housing is designed to reduce acoustic energy associated with compressor intake flow. Molded from aerospace quality fiberglass, the intake suppressor mounts to the SR-30 engine with a pneumatic friction seal system. The exhaust suppressor assembly is manufactured from stainless steel to maximize heat dissipation and durability. A positive pressure clamping system requires no modification of the existing Minilabs for installation. The suppressor exhaust ducting incorporates a glass sight window for flame plume visibility during starting operation. An acoustic expansion chamber on the end of the duct provides a convenient transition to facility specific exhaust ducting and integrates well with already existing installations[12].

4.8 Hush kit Specification

A hush kit complete sound suppression system designed to reduce both engine core and jet noise, Inlet suppressor manufactured from molded fiberglass, Exhaust suppressor manufactured from stainless steel, Exhaust suppressor duct to be equipped with flame plum viewing window, Inlet and exhaust assemblies to be readily removable to allow access to engine, Inlet and exhaust assemblies to be mounted in such a way as to not interfere with any operation of the engine, To require no modifications of existing Minilab unit, Provided with a comprehensive installation and usage instructions[12].

5 Experimental Preparation and Procedure

The central work within this project objectives are to run and evaluate the performance of the SR-30 microturbine and also the installation and operational experience with the SR-30 microturbine is described. The installation included providing the necessary utilities, building a suction pipe flange for installation of air heater and building an exhaust manifold for exhaust gas expulsion.

The data acquisition system is provided using a PC and software allowing continuous display of measurements from the SR-30 microturbine. The measurements available allow for the calculation of component efficiencies, compressor, turbine power and thermal efficiency at various power settings.

5.1 SR-30 Microturbine Installation and Set Up

The design of the components is typical for a jet engine of this compact size as it incorporates a radial compressor and has a change in flow direction in the annular, reverse flow combustion chamber. The installation had to be such as to avoid permanent alterations of the building exterior. Hence, the installation process demanded more planning and energy than that foreseen for a normal lab situation. The system includes the auxiliary subsystems required for the operation of the SR-30 engine. These include fuel, lubrication and ignition subsystems.

The SR-30 requires a source of 100 bar compressed air for starting the engine. However, it is not suitable for indoor operation as delivered because of the noise and exhaust gases. The noise level can be reduced by adding an acoustical intake manifold and a dual pipe insulated exhaust. The exhaust system directs the exhaust gases out of the laboratory building.

To avoid a permanent building modification, while allowing operation during all weather conditions, I used exhaust system which is already available in the laboratory and connected with microturbine. The insulated pipe flange is connected to the inlet system of the turbine and also the external compressor connected to supply air pressure up to 100 bar with a sustainable pressure of 80 bar.

Figure 5.1 Turbine Intake and Exhaust System

Source: Author

All of the system controls are on the operator panel where the engine can be started by a single push button. This panel also monitors the values of turbine inlet temperature, exhaust gas temperature and speed are monitored. In addition, the pressures in the air, fuel and oil supply are measured and compressor exit pressure is indicated.

Figure 5.2 Intake manifold Connection

Source: Author

Figure 5.2 shows intake manifold connection. One side of the insulated pipe flange is connected to the turbine and another side is connected to the outside environment. From this we can get higher mass flow rate of air through the turbine.

Figure 5.3 Air Heater Connection

Source: Author

Figure 5.3 shows Air heater connection. Here, another side of the insulated pipe flange is connected to the air heater it will allow us to heat the intake air temperature and leads to analysis of the device's efficiency on the intake air temperature.

5.2 Operational Facts of the SR-30 Microturbine

The starting of the turbine is the most striking phase, and it requires a proper physical coordination. Prior to the test, the fuel, lubricating and compressed air systems were checked to make sure those systems are functioning properly and adequately supplied for the tests planned. The compressed air is employed to activate the turbine, and the engine operates satisfactorily using a variety of fuels, I used diesel fuel to operate the turbine.

5.2.1 Operating Procedure

The external compressor is connected with microturbine and the power cord plugged into a wall outlet, and the system is ready for testing.

Figure 5.4 Turbine Test System

Source: Author

After turning on the master key switch and electronic master switch then the LED displays were switched on automatically. For reading the measurement data acquisition system provided using a pc and software allowing continuous display of measurements from the SR-30 microturbine. The ignitor is switched on and its functioning verified. The throttle is pushed into the wide-open position.

The compressed air is employed to activate the turbine, When the rotational speed of the engine reaches a specific value, the fuel pump is turned on and the ignition occurs. The engine speed increases rapidly. Upon ignition, flames are visible in the exhaust, and they disappear as the throttle is pushed back to idle. The exhaust gas temperature was monitored.

5.2.2 Abnormal Start and Flag Indication

During SR-30 microturbine test run some of the starts did not result in ignition and hung start and fuel leakage were detected. So, the turbine was removed and checked for identify the problem.

Figure 5.5 SR-30 Fuel Valve Operating System

Source: Author

The reason for the abnormal start it's because of the hung start and it leads to fuel leakage after detecting fuel leakage fuel switch was turned off and turbine fuel valve operating system was dismantled and performed several air cleanings.

After some test run, I identified the cause for the hung start it's because of insufficient fuel pressure so, I set the fuel pressure to 150 bar and then the engine run without any problem. I restarted turbine by following normal operating procedure and the it was run properly and the temperature were measured.

6 SR-30 Microturbine Measured Data

The SR-30 engine was run several times on this project to test the engine intake air efficiency at different temperature and by using Data acquisition software, we measure Gas Turbine Run Data in preparation for system analysis and performance calculations. During starting stage of the engine run there is a gap of time where temperature variations are observed these temperatures are dependent on the starting condition of the engine. The measured data is helps us to calculate the air mass flow rate, compressor and turbine isentropic efficiencies, air fuel ratio, specific fuel consumption etc.,

In this project engine had been run and tested for six start up conditions. The engine data was measured for different temperature. The cold start was a normal start and after a first run engine had been kept for idle condition. All engine components were at room temperature. By using external compressed air, the engine was then cooled by drawing in room temperature air and those component temperatures were monitored.

6.1 Turbine Testing Data

The SR-30 turbojet engine operating at steady state for six different operating speeds over the range of 68,000 to 76,000 rpm and the test data was measured for six different temperatures.

Time	**Speed**	**Comp in T**
	N	**T_1**
	(rpm)	***(°C)***
15:08:52	76438.8	39.48
15:41:24	71121.7	52.81
15:59:56	68688.2	42.95
16:16:54	69537.3	47.42
18:08:57	74540.5	5.48
18:17:50	74564.3	5.2

Table 6.1 Inlet air temperature, Speed

Source: Author

Table 6.1 represents the measured data of inlet air temperature and various engine speed which is measured according to different time interval.

Atm. Pressure	Heating Fuels	Fuel Density
(kPa)	***(kJ/kg)***	***(kg/m3)***
102	42610	0.81

Table 6.2 Fuel Density and Calorific Value

Source: Author

The atmospheric pressure, fuel density and the calorific value of the working fuel are shown in Table 6.2.

6.1.1 Low Temperature Measurement

The SR-30 combustion turbine intake air was measured for two different low temperatures. The temperatures were measured at different turbine speed and the pressure difference of inlet, outlet of the compressor and turbine was monitored.

Time	Comp in	Comp exit	Turb in	Turb exit	Nozzle exit	Fuel flow	Speed	Comp in T
	P_1	P_2	P_3	P_4	P_5	m_p	N	T_1
	(kPa)	***(kPa)***	***(kPa)***	***(kPa)***	***(kPa)***	***(l/h)***	***(rpm)***	***(°C)***
18:08:57	2.66	175.46	175.29	27.05	19.79	22.61	74540.5	5.48
18:17:50	2.63	175.58	175.43	27.29	20.05	23.32	74564.3	5.2

Table 6.3 Fuel Flow, Pressure Difference at Low Temperature

Source: Author

Table 6.4 represents the inlet, outlet of the compressor and turbine temperatures and the exhaust gas temperatures are measured at different engine speed. Those all-temperatures differences were measured at low temperature.

Speed	Comp in T	Comp ex T	Turb in T	Turb ex T	EGT
N	T_1	T_2	T_3	T_4	T_{ex}
(rpm)	*(°C)*	*(°C)*	*(°C)*	*(°C)*	*(°C)*
74540.5	5.48	155.57	740.79	585.78	454.91
74564.3	5.2	161.81	744.42	586.84	460.61

Table 6.4 Exhaust Temperature, Temperature Difference at Low Temperature

Source: Author

6.1.2 High Temperature Measurement

The SR-30 combustion turbine intake air was measured for four different high temperatures. Compared with low temperature measurement the turbine run at mostly in high temperature and the Table 6.5 shows fuel flow, pressure difference between inlet, outlet of the compressor and turbine.

Time	Comp in	Comp exit	Turb in	Turb exit	Nozzle exit	Fuel flow	Speed	Comp in T
	P_1	P_2	P_3	P_4	P_5	m_p	N	T_1
	(kPa)	*(kPa)*	*(kPa)*	*(kPa)*	*(kPa)*	*(l/h)*	*(rpm)*	*(°C)*
15:08:52	2.41	155.1	156.06	23.56	16.88	24.58	76438.8	39.48
15:41:24	1.91	120.57	122.63	19.24	11.83	23.98	71121.7	52.81
15:59:56	1.63	109.25	111.8	17.64	10.2	23.93	68688.2	42.95
16:16:54	1.72	111.64	113.74	18.01	10.25	23.95	69537.3	47.42

Table 6.5 Fuel Flow, Pressure Difference at High Temperature

Source: Author

Speed	Comp in T	Comp ex T	Turb in T	Turb ex T	EGT
N	**T_1**	**T_2**	**T_3**	**T_4**	**T_{ex}**
(rpm)	***(°C)***	***(°C)***	***(°C)***	***(°C)***	***(°C)***
76438.8	39.48	231.53	886.32	736.64	600.47
71121.7	52.81	214.62	860.84	731.92	588.02
68688.2	42.95	194.86	837.13	715.53	576.82
69537.3	47.42	198.75	853.03	725.73	588.06

Table 6.6 Exhaust Temperature, Temperature Difference at Low Temperature

Source: Author

Table 6.6 shows that temperature difference between inlet, outlet of the compressor and turbine and the exhaust gas temperature of the turbine. The turbine runs at different speed over the range of 68,000 to 76,000 and compared with low temperature measurement, high temperature measurement exhaust gas is very high.

7 Computation of SR-30 Microturbine

On the basis of SR-30 microturbine measured data, the thermodynamic calculation is calculated. To study about proper working principle and turbine efficiency, the computation of turbine will help us to calculate the enthalpy of the working substance in the basic points of thermal circulation, specific work of compressor and turbine, mass flow of the working substance, thermodynamic efficiency etc.,

7.1 Determination of Enthalpies

The specific heat capacity at constant pressure for air of a given temperature is

$$\boldsymbol{i_{vz} = (-0.1 \times 10^{-16} \times t^5 + 0.3 \times 10^{-12} \times t^4 - 0.7 \times 10^{-19} \times t^3)} \qquad \textbf{(7.1)}$$

To determine the enthalpies of the working substance in the basic points of heat above mentioned equation is used to calculate specific heat capacity where enthalpy i_{vz} and inlet, outlet temperature difference(t) of the compressor and turbine, Table 7.1 illustrates the calculated values according to measured data of SR-30 microturbine.

Comp in T_1	**i_1**	**i_2**	**i_3**	**i_4**
(°C)	**(kJ/kgK)**	**(kJ/kgK)**	**(kJ/kgK)**	**(kJ/kgK)**
39.48	39.68	238.25	1037.24	838.41
52.81	53.11	220.20	1002.60	832.30
42.95	43.17	199.27	970.69	811.17
47.42	47.68	203.37	992.06	824.31
5.48	5.50	158.14	843.78	647.62
5.2	5.22	164.63	848.49	648.93

Table 7.1 Determination of Enthalpies

Source: Author

7.2 Turbo compressor

$$\boldsymbol{a_K = \Delta i = i_2 - i_1} \qquad \textbf{(7.2)}$$

Indoor work corresponds to a change in the state of the air where a_k is the compressor work and Δi is the enthalpy difference. Ideal work of the compressor a_{Kie} is calculated by:

$$a_{Kie} = \Delta_i = i_{2,ie} - i_1 \quad (7.3)$$

The indoor work corresponds to a change in the state of the air and also heat sharing with the environment is negligible.

$$T_{2,ie} = T_1 \times \left(\frac{p_2}{p_1}\right)^{\frac{0.4}{1.4}} \quad (7.4)$$

The ideal outlet temperature $T_{2,ie}$ is lower. P_2, P_1 is the inlet and outlet of the compressor pressure. Table 7.2 shows about the calculation of the compressor work.

a_K *(KJ/Kg)*	a_{Kie} *(KJ/Kg)*	$T_{2,ie}$ *(°C)*
198.57	93.34	131.28
167.09	80.71	132.06
156.09	72.39	114.29
155.70	74.70	120.93
152.64	90.35	94.98
159.41	90.33	94.69

Table 7.2 Calculation of The Compressor Work

Source: Author

7.3 Specific Work of The Turbine

$$a_T = \Delta i = i_3 - i_4 \quad (7.5)$$

Indoor work corresponds to a change in the state of the air where a_T is the turbine work and Δi is the enthalpy difference. Ideal work of the turbine a_{Tie} is calculated by:

$$a_{Tie} = \Delta_i = i_{3,ie} - i_4 \quad (7.6)$$

The indoor work corresponds to a change in the state of the air and also heat sharing with the environment is negligible.

$$T_{4,ie} = T_3 \times \left(\frac{p_4}{p_3}\right)^{\frac{0.4}{1.4}} \quad (7.7)$$

The ideal outlet temperature $T_{4,ie}$ is lower. P_4, P_3 is the inlet and outlet of the turbine pressure. Table 7.3 shows about the calculation of the turbine work.

a_T (KJ/Kg)	a_{Tie} (KJ/Kg)	$T_{4,ie}$ (°C)
198.83	283.42	670.62
170.30	239.87	677.65
159.52	220.93	667.43
167.75	227.25	679.28
196.16	250.13	541.75
199.56	250.91	544.98

Table 7.3 Calculation of The Turbine Work

Source: Author

7.4 Mass Flow

$$\boldsymbol{m_{vz} = w_{vz} \times s_k \times \rho_{vz}} \quad \textbf{(7.8)}$$

Where, m_{vz} is the amount of inlet air, turbocharger suction flow cross section S_K = 0.00311 m^2.

$$\boldsymbol{\rho_{vz} = \rho_{vz,N} \times \frac{p_1}{p_n} \times \frac{T_N}{T_1}} \quad \textbf{(7.9)}$$

Constant air density $\rho_{vz,N} = 1.293\ kg/m^3$, $p_1$is the inlet compressor pressure, $p_n$is the atmospheric air pressure and the T_1, T_N is the compressor inlet temperature and constant temperature.

$$\boldsymbol{w_{vz} = \sqrt{\frac{2 \times p_1}{p_{vz}}}} \quad \textbf{(7.10)}$$

Where, w_{vz} is the intake air speed, p_1 is the inlet compressor pressure.

m_{vz} $(kg.s^{-1})$	ρ_{vz} $(kg.m^{-3})$	w_{vz} $(m.s^{-1})$
0.23	1.16	64.35
0.20	1.11	58.63
0.19	1.14	53.41
0.19	1.13	55.23
0.26	1.31	63.74
0.26	1.31	63.36

Table 7.4 Mass Flow of The Working Substance

Source: Author

7.5 Compressor and Turbine Power

$$P_K = m_{vz} \times a_K \quad (7.11)$$

$$P_{Kie} = m_{vz} \times a_{Kie} \quad (7.12)$$

The compressor power P_K, P_{Kie} are calculated by the product of inlet air with compressor work.

$$P_T = m_{vz} \times a_T \quad (7.13)$$

$$P_{Tie} = m_{vz} \times a_{Tie} \quad (7.14)$$

The turbine power P_T, P_{Tie} are calculated by the product of inlet air with turbine work.

P_K *(KW)*	P_{Kie} *(KW)*	P_T *(KW)*	P_{Tie} *(KW)*
46.26	21.74	46.32	66.02
33.85	16.35	34.51	48.60
29.63	13.74	30.28	41.93
30.16	14.47	32.50	44.02
39.62	23.45	50.92	15.36
41.16	23.32	51.52	64.77

Table 7.5 Compressor and Turbine Power

Source: Author

7.6 Fuel Consumption

$$\boldsymbol{q_a = \Delta i = i_3 - i_2} \quad \textbf{(7.15)}$$

In the combustion chamber the pressure loss is negligible. The fuel input is equal to heat supplied to the combustion chamber. Table 7.6 shows that the calculation of q_a.

$\mathbf{q_a}$ $(\boldsymbol{kJ.kg^{-1}})$
798.99
782.41
771.43
788.69
685.64
683.86

Table 7.6 Calculation of q_a

Source: Author

7.7 Thermodynamic Efficiencies

$$\boldsymbol{\eta_{kie} = \frac{a_{kie}}{a_k} \times 100} \quad \textbf{(7.16)}$$

Where, η_{kie} is the thermodynamic efficiency of the compressor and a_{kie}, a_k are the output and input compressor work done.

$$\boldsymbol{\eta_{Tie} = \frac{a_{Tie}}{a_T} \times 100} \quad \textbf{(7.17)}$$

Where, η_{Tie} is the thermodynamic efficiency of the turbine and a_{Tie}, a_T are the output and input turbine work done.

$$\boldsymbol{\eta_{total} = \frac{a_0}{q_a} \times 100} \quad \textbf{(7.18)}$$

Where, η_{total} is the thermodynamic efficiency of the whole circulation and a_0, q_a are the work done and the fuel supply of the whole turbine system.

Speed N *(rpm)*	**Comp in T1** *(°C)*	**η_{kie}** *(%)*	**η_{tie}** *(%)*	**η_{total}** *(%)*
76438.8	39.48	47.01	70.15	0.03
71121.7	52.81	48.30	71.00	0.41
68688.2	42.95	46.38	72.21	0.44
69537.3	47.42	47.98	73.82	1.53
74540.5	5.48	59.19	78.42	6.35
74564.3	5.2	56.66	79.54	5.87

Table 7.7 Thermodynamic Efficiency Calculations

Source: Author

Table 7.7 shows about the thermodynamic efficiency of compressor, turbine and the overall device efficiency. All the values were measured and calculated with respect of intake air temperature.

8 Results

The SR-30 microturbine run data were collected at six engine speeds ranging from 68,000 to 76,000 rpm. First four data were measured at high temperature and two of them at low temperature. All data from turbine measured at fixed engine speed, with the help of data acquisition system the turbine data was monitored.

The measured data were evaluated in the previous chapter and analyze the engine performance. The engine performance is related to the speed and the components efficiencies. One of the independent variables when conducting tests with this engine system is the engine speed. The results of evaluated data help us to understand the thermodynamic properties and engine efficiency, results will also be evaluated at a specific speed in order to illustrate what happens to the fluid throughout the microturbine.

The evaluated values can be presented graphically, it illustrates the thermodynamic properties, air mass flowrate, compressor, turbine, device efficiencies. The graphical representation shows us to understand the performance characteristics of engine clearly. the engine was run for several times and data were recorded. This shows that the heating of the component of the engine with respect to time, it is less impact and thus a steadier temperature state can be reached in a shorter period of time.

The six different measured data from turbine run which is measured at different temperature all operations are conducted at study state and are averaged to calculate turbine parameters. This parameter shows the operation of the turbine are calculated using stagnation conditions, which are easily determined with the knowledge of air and fuel flow of the cross section of the turbine.

All engine set up were at room temperature. The hot starts were actually restarting, after the engine had been operating. The engine was operated according to the operating procedure so, after the working operation the engine was shut down with standard operating procedures. The external compressed air supply used to spin the compressor turbine spool, the engine was then cooled by drawing in room temperature air, then the engine component temperatures were monitored during this period.

8.1 Fuel Flow Rate

The fuel flow rates increase almost linearly as the microturbine speed increases. Figure 8.1 shows about graphical representation of fuel flow and speed.

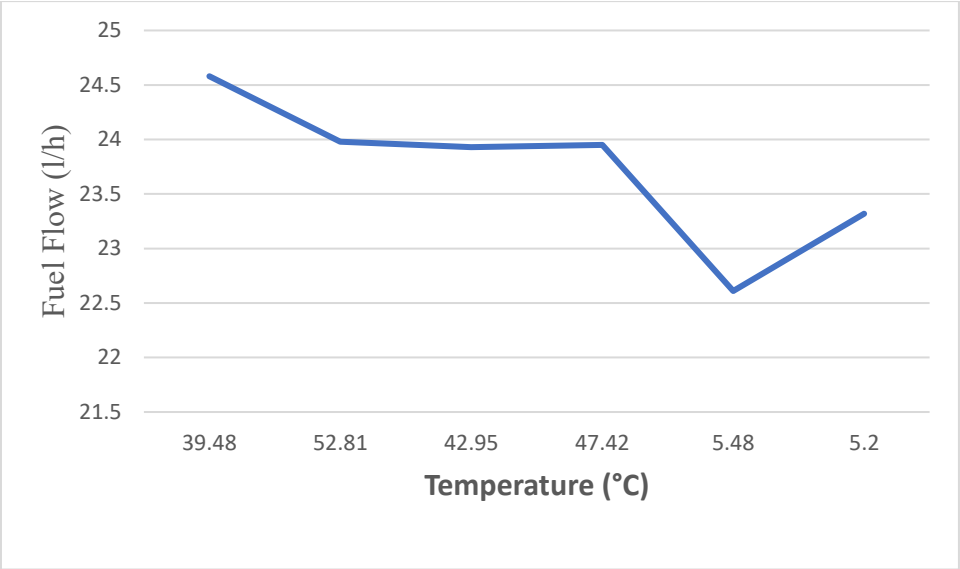

Figure 8.1 Fuel Flow Versus Temperature

Source: Author

The plotted graphical representation illustrates about temperature ratio at the range of 5.48 *°C* the fuel flow also has low value around 22.61 *l/h*. when the temperature of the intake air increases around 39.48 *°C* the fuel flow rate also slightly increased to 24.58 *l/h*.

Comp in T	**Fuel flow**
T_1	**m_p**
(°C)	***(l/h)***
39.48	24.58
52.81	23.98
42.95	23.93
47.42	23.95
5.48	22.61
5.2	23.32

Table 8.1 Fuel Flow Versus Temperature

Source: Author

8.2 Pressure Ratio

Figure 8.2 illustrates about graphical representation of microturbine components pressure difference with respect to speed.

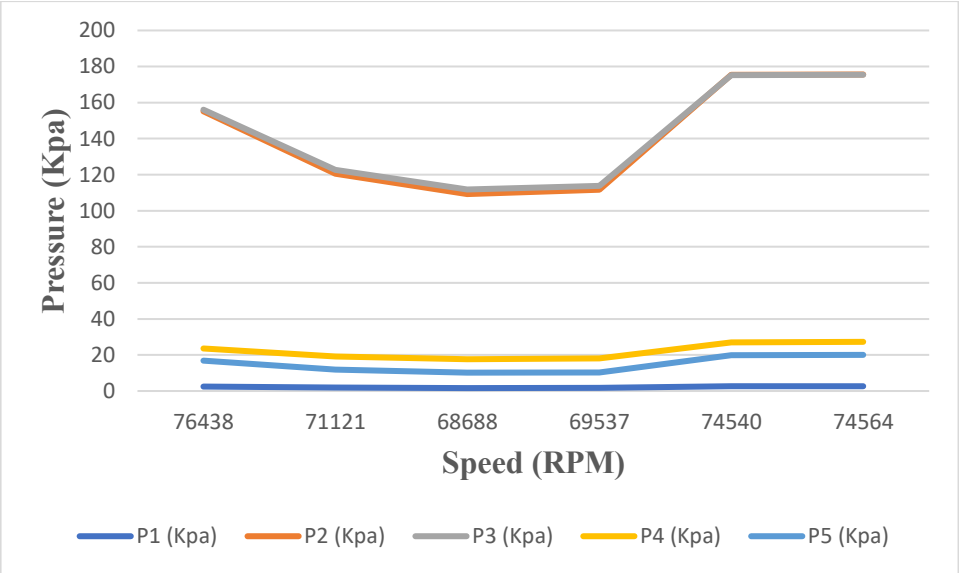

Figure 8.2 Pressure Ratio Versus Speed

Source: Author

The compressor inlet pressure ratio (P_1) for the speed range of 68,688 rpm is low its pressure is around 1.63 *kPa* and for speed 76,438 rpm the compressor inlet pressure is high it's about 2.41 *kPa*. For the low temperature measurement, the compressor outlet pressure ratio is higher with high-speed engine run. For the high temperature measurement, the compressor outlet pressure ratio is lower with low-speed engine run. The compressor outlet pressure (P_2) for the speed 74,540 rpm its pressure is about 175.46 *kPa* and the low-speed range around 68,688 rpm and its pressure has 109.25 *kPa*.

The turbine inlet pressure ratio (P_3) for the speed range of 68,688 *rpm* is low its pressure is around 111.8 *kPa* and for speed 74,564 *rpm* the turbine inlet pressure is high it's about 175.43 kPa. The turbine outlet pressure (P_4) for the speed 74,564 rpm the pressure reaches about 27.29 kPa and the low-speed range around 68,688 rpm has 17.64 *kPa* pressure.

The nozzle exit pressure ratio (P_5) for the speed range of 68,688 rpm is low and the pressure range is 10.25 k*Pa* and for the low temperature measurement, for the speed of 74,564 *rpm* the pressure reaches around 20.05 *kPa*.

Speed (N)	P_1	P_2	P_3	P_4	P_5
(rpm)	*(kPa)*	*(kPa)*	*(kPa)*	*(kPa)*	*(kPa)*
76438	2.41	155.1	156.06	23.56	16.88
71121	1.91	120.57	122.63	19.24	11.83
68688	1.63	109.25	111.8	17.64	10.2
69537	1.72	111.64	113.74	18.01	10.25
74540	2.66	175.46	175.29	27.05	19.79
74564	2.63	175.58	175.43	27.29	20.05

Table 8.2 Pressure Ratio Versus Speed

Source: Author

8.3 Temperature Ratio

Figure 8.3 shows about graphical representation of microturbine components temperature difference with respect to speed.

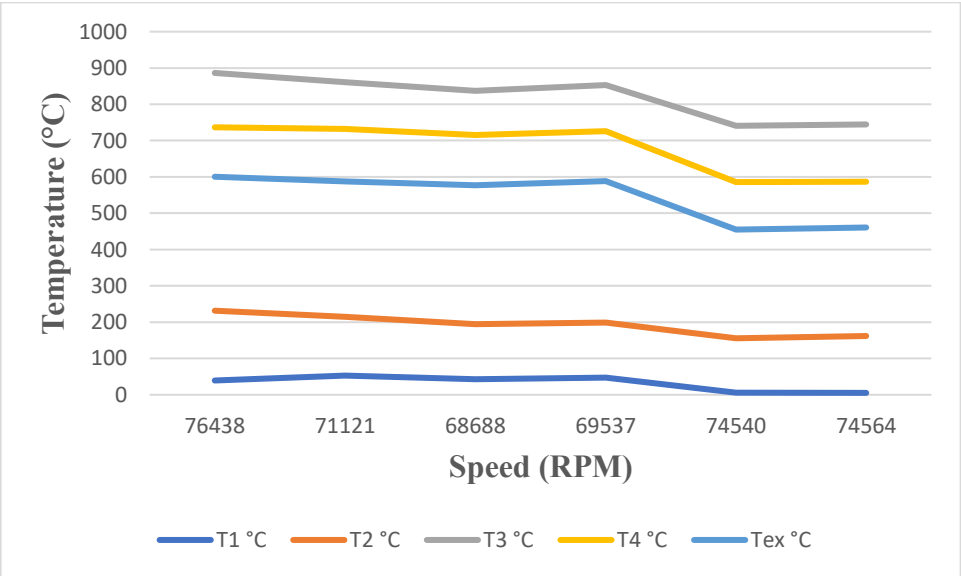

Figure 8.3 Temperature Ratio Versus Speed

Source: Author

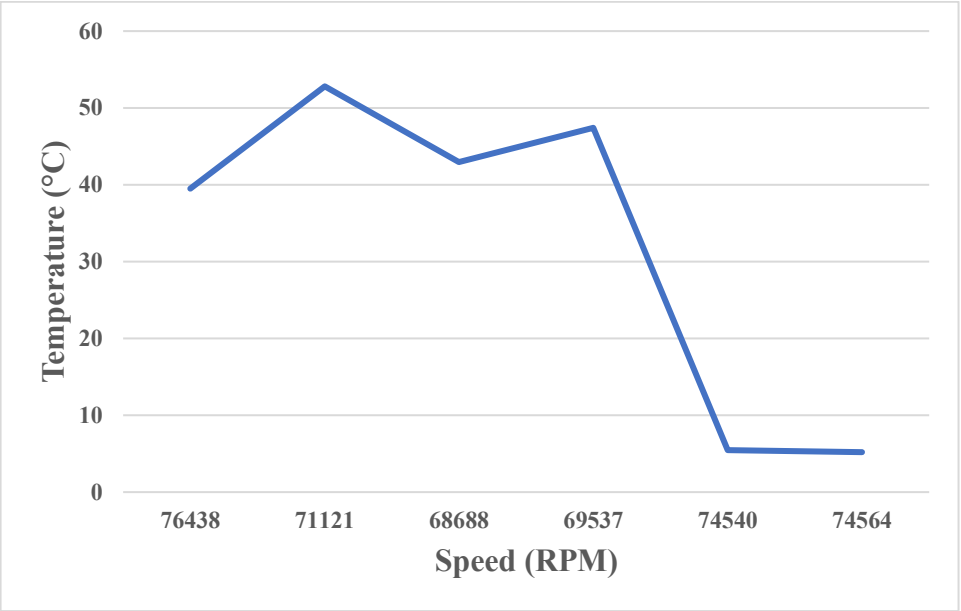

Figure 8.4 Compressor Inlet Temperature Versus Speed

Source: Author

The temperature (T_1) is the compressor inlet temperature, the measured data for the temperature (T_1) for the low temperature range, the speed of the engine is ranges from 74,540 to 74,564 *rpm* and for the high temperature measured data the engine speed it's up to 71,121 rpm.

The temperature (T_2) is the compressor outlet temperature, for the measured data for the temperature (T_2) the speed of the engine is around 74,540 to 74,564 *rpm*. The temperature ratios for temperature (T_2) have low values it's around 155.57 to 161.81 *°C*. And for the high temperature measured data the engine speed it's up 76,438 rpm and its temperature values are around 231.53 *°C*.

The temperature (T_3) is the turbine inlet temperature, the measured data for the temperature (T_3) the speed of the engine is around 74,540 to 74,564 rpm. The temperature ratios for temperature (T_3) have low values it's around 740.79 to 744.42 *°C*. And for the high temperature measured data the engine speed it's up 76,438 rpm and its temperature values are around 886.32 *°C*. The turbine outlet temperature (T_4) also has the values not as much higher than turbine inlet temperature.

Speed	T_1	T_2	T_3	T_4	T_{ex}
(rpm)	*(°C)*	*(°C)*	*(°C)*	*(°C)*	*(°C)*
76438	39.48	231.53	886.32	736.64	600.47
71121	52.81	214.62	860.84	731.92	588.02
68688	42.95	194.86	837.13	715.53	576.82
69537	47.42	198.75	853.03	725.73	588.06
74540	5.48	155.57	740.79	585.78	454.91
74564	5.2	161.81	744.42	586.84	460.61

Table 8.3 Temperature Ratio Versus Speed

Source: Author

The exhaust gas temperature (T_{ex}), has the low temperature value for the speed of 74,564 rpm and it has higher temperature value for the speed of 76,438 *rpm*.

8.4 Compressor and Turbine Work

Figure 8.5 illustrates about graphical representation of compressor work with respect to speed.

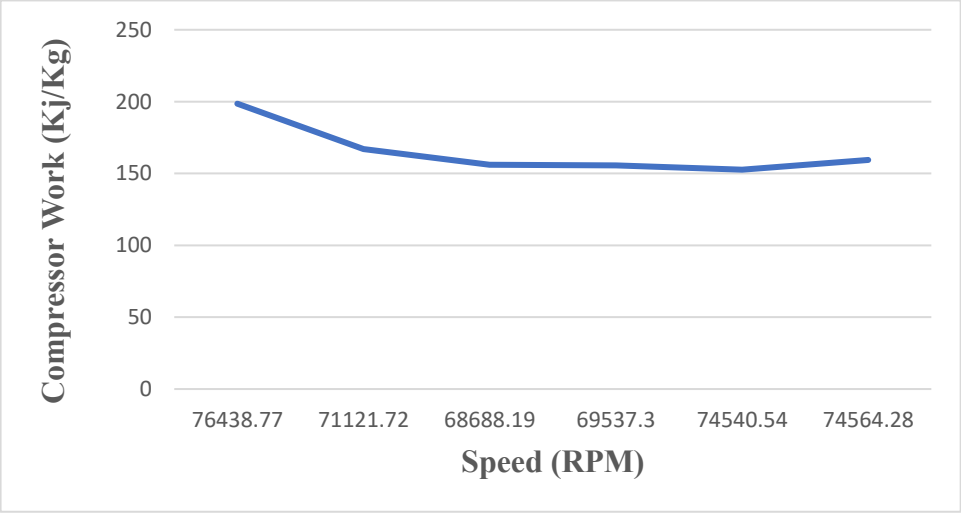

Figure 8.5 Compressor Work Versus Speed

Source: Author

For the speed of 69,537 rpm the compressor work, it was recorded as low value of the work is 155.7 *kJ/kg* and 198.57 *kJ/kg* were recorded for the speed of 76,438 *rpm* and it is the highest work done of the compressor.

Figure 8.6 illustrates about graphical representation of turbine work with respect to speed.

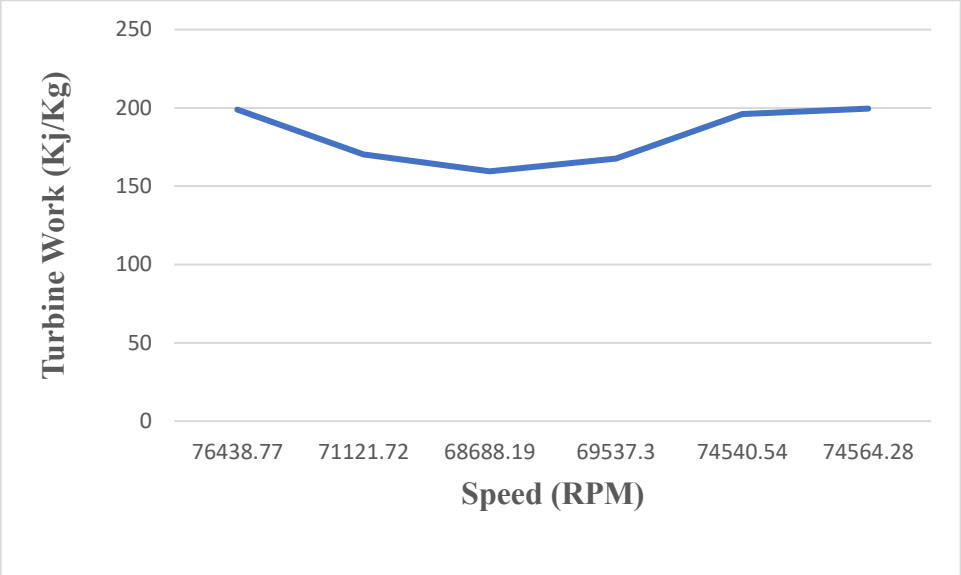

Figure 8.6 Turbine Work Versus Speed

Source: Author

For the speed of 68,688 rpm the turbine work, it was recorded as low value of the work is 159.52 k*J/kg* and 199.56 kJ/*kg* were recorded for the speed of 74,564 *rpm* and it is the highest work done of the compressor.

Speed (N)	a_k (kJ/*kg*)	a_T (kJ/*kg*)
76438.77	198.57	198.83
71121.72	167.09	170.3
68688.19	156.09	159.52
69537.3	155.7	167.75
74540.54	152.64	196.16
74564.28	159.41	199.56

Table 8.4 Compressor and Turbine Work Versus Speed

Source: Author

8.5 Component Efficiencies

Figure 8.7 shows about graphical representation of work of compressor efficiency with respect to temperature. At temperature 5.48 $°C$ the improved compressor efficiency was attained; the efficiency reaches around 59.1 $\%$ and the lowest efficiency value of compressor efficiency was obtained at the temperature 42.95 $°C$ and the efficiency value is 46.38 $\%$.

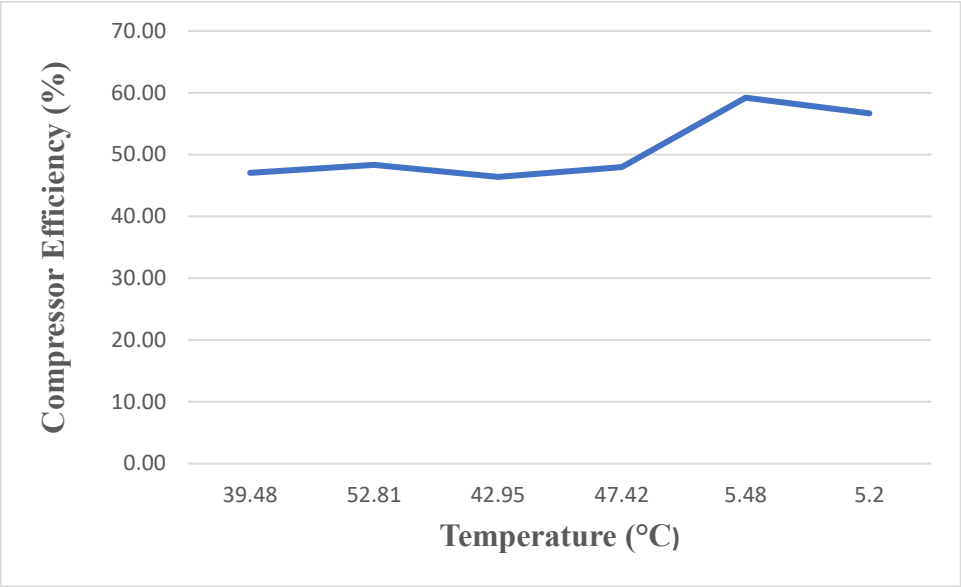

Figure 8.7 Compressor Efficiency Versus Temperature

Source: Author

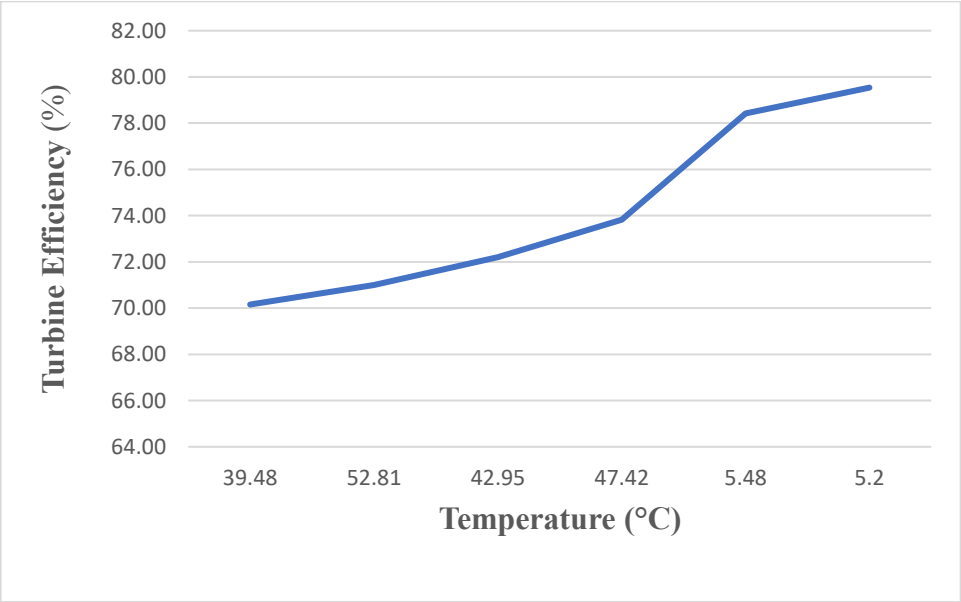

Figure 8.8 Turbine Efficiency Versus Temperature

Source: Author

Figure 8.8 illustrates about graphical representation of work of turbine efficiency with respect to temperature. At temperature 5.2 *°C* the improved turbine efficiency was attained; the efficiency reaches around 79.54 *%* and the lowest efficiency value of turbine efficiency was obtained at the temperature 39.48 *°C* and the efficiency value is 70.15 *%*.

Comp in T_1	**η_{kie}**	**η_{tie}**	**η_{total}**
(°C)	***(%)***	***(%)***	***(%)***
39.48	47.01	70.15	0.03
52.81	48.3	71	0.41
42.95	46.38	72.21	0.44
47.42	47.98	73.82	1.53
5.48	59.19	78.42	6.35
5.2	56.66	79.54	5.87

Table 8.5 Thermodynamic Efficiency Versus Temperature

Source: Author

Figure 8.9 illustrates about graphical representation of work of overall device efficiency with respect to temperature. At temperature 5.48 *°C* the improved overall device efficiency was attained; the efficiency reaches around 6.35 *%* and the lowest efficiency value of overall device efficiency was obtained at the temperature 39.48 *°C* and the efficiency value is 0.03 *%*.

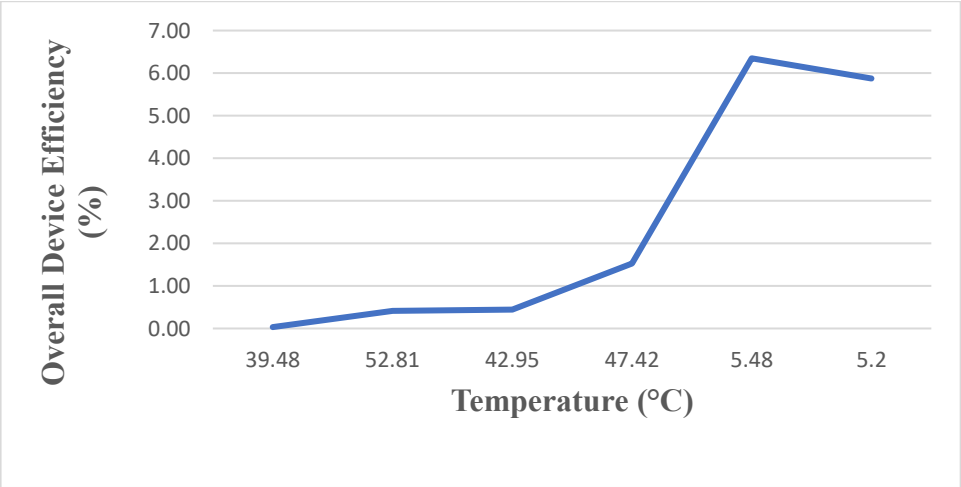

Figure 8.9 Overall Device Efficiency Versus Temperature

Source: Author

9 Correlation Analysis

This section gives the analytical solution to the engine performance. In the previous section's performance of SR-30 microturbine was determined from the measured data and those data were calculated and plotted for study about the engine performance by monitoring several data.

Correlation analysis was performed to analyze the calculated data. Correlation analysis is the method used to evaluate the two variables and it will analyze and provide the probabilities of several variable data statistically. In this project the method correlation analysis is used to analyze the device efficiency on intake air temperature.

To perform the correlation analysis there are so many software can be used for example EXCEL, ENGINEERING EQUATION SOLVER, MAT LAB etc., I used mat lab to perform the correlation analysis, mat lab helps to analyze the complicated equations. Here all the measured data of SR-30 microturbine were implemented on the mat lab and measured parameters were carefully correlated and analyzed with device efficiency on intake air temperature and all the analyzed values were plotted graphically with respect to temperature and efficiency.

One of the main reasons for doing correlation analysis is to analyze the probable variables of turbine efficiency with different intake air temperature input because in this project there were six different temperature was measured and calculated in those six three of the values are hot temperature measurement and two of them are cold temperature measurements. Compared with hot temperature measurement the cold temperature values has high turbine efficiencies. So, in some point whenever the climatic conditions are not suitable to measure the data in that point correlation analysis method will gives the analyzed result.

Performing correlation analysis in mat lab helps us to change the all parameters in comparison with others. Previously the measured data were evaluated in excel and the data from excel was imported to mat lab and performed an analysis process. According to evaluated value from measured data the overall device efficiency is very low for the hot temperature measurement but cold temperature measurement value efficiencies are slightly increasing so, in the correlation analysis process the main temperature values are going to be reduced to low temperature value and compared with calculated efficiency values.

9.1 Temperature Analysis

Figure 9.1 shows about graphical representation of correlation analysis of temperature which is analyzed in mat lab.

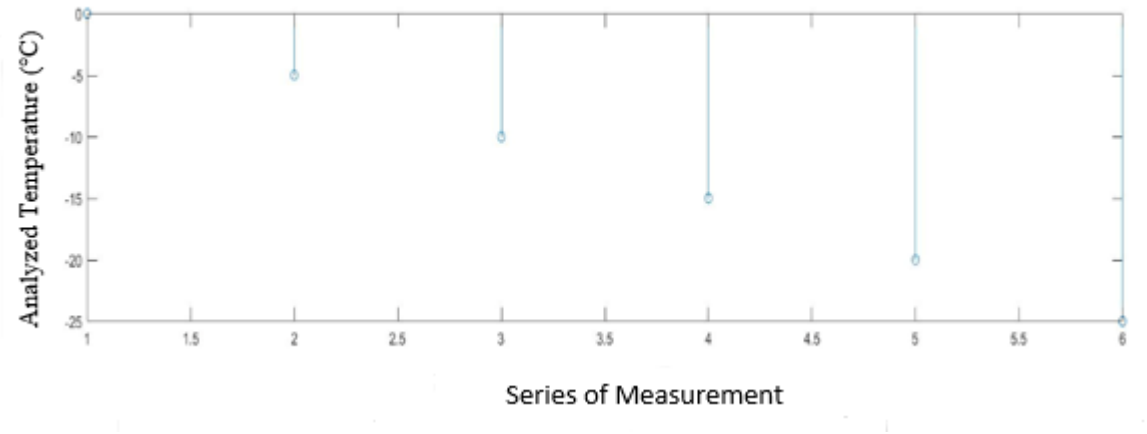

Figure 9.1 Correlation Analysis of Temperature

Source: Author

The measured intake air temperature of the SR-30 microturbine is higher than analyzed temperature. In measured intake air temperature are ranges from 40 to 52 *°C* are high values the lower values are ranges from 5.2 to 5.48 *°C* which has the high device efficiency output when compared with high temperature measurement.

Measured Intake Air Temperature	**Analyzed Intake Air Temperature**
(°C)	***(°C)***
39.48	0
52.81	-5
42.95	-10
47.42	-15
5.48	-20
5.2	-25

Table 9.1 Temperature Comparison

Source: Author

Table 9.1 shows about the comparison of measured and analyzed intake air temperature. Those analyzed temperature values are took from mat lab correlation analysis process. During correlation analysis the values are analyzed with low temperature value because the measured temperatures are so high and the device efficiency of the measured values are so low.

9.2 Efficiency Analysis

Figure 9.2 shows about graphical representation of correlation analysis of efficiency

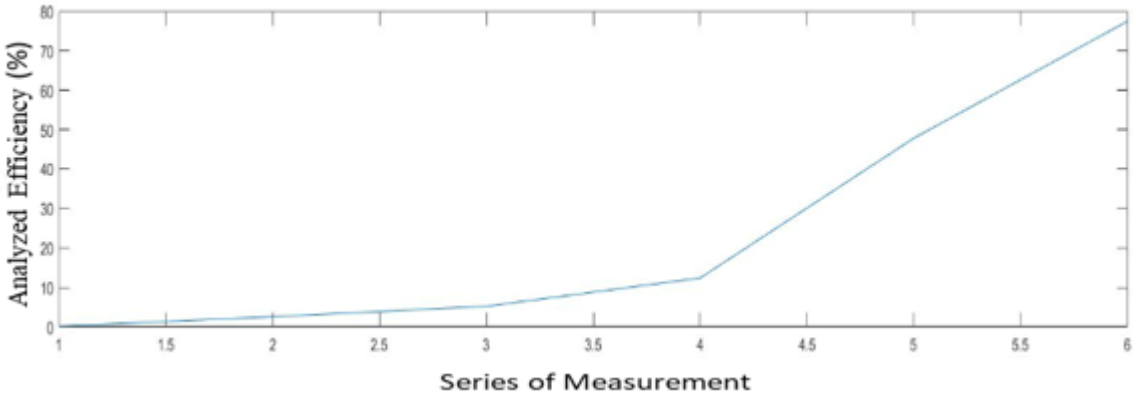

Figure 9.2 Correlation Analysis of Efficiency

Source: Author

The evaluated value of overall device efficiency from measured data is too less because of the values of intake air temperature are high and the analyzed efficiency values are higher than evaluated efficiency value because these values are correlated with respect to correlated intake air temperature.

Calculated Efficiency (η_{total})	**Analyzed Efficiency (η_{total})**
(%)	***(%)***
0.03	0.1761
0.41	2.5972
0.44	5.2322
1.53	12.4156
6.35	47.8559
5.87	77.4829

Table 9.2 Efficiency Comparison

Source: Author

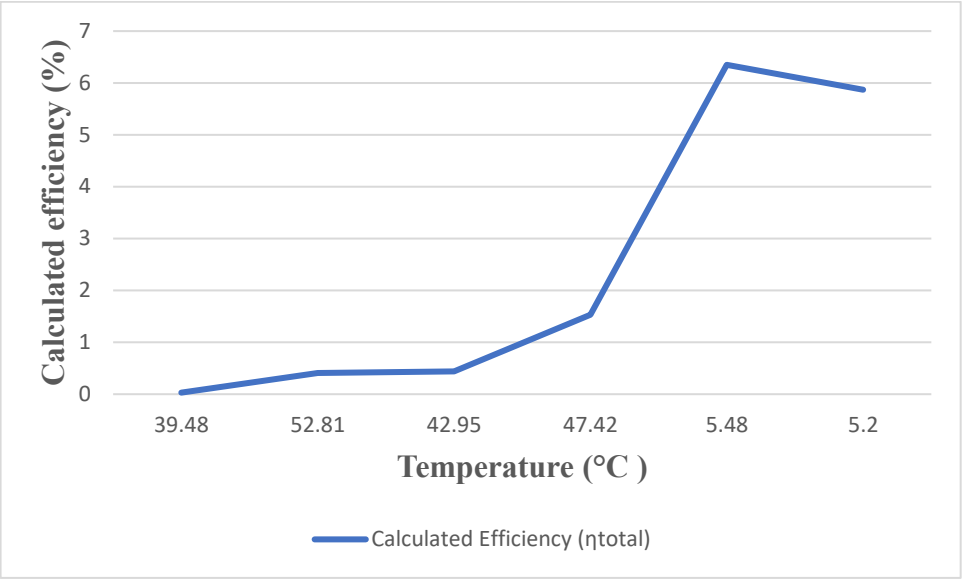

Figure 9.3 Calculated Efficiency

Source: Author

Figure 9.3 illustrates about graphical representation of calculated overall device efficiency with respect to intake air temperature. Figure 9.4 illustrates about graphical representation of analyzed overall device efficiency with respect to intake air temperature. Here, the correlated analyzed value efficiency is more efficient the highest efficiency value is 77.48 % and the lowest value is 0.176 %

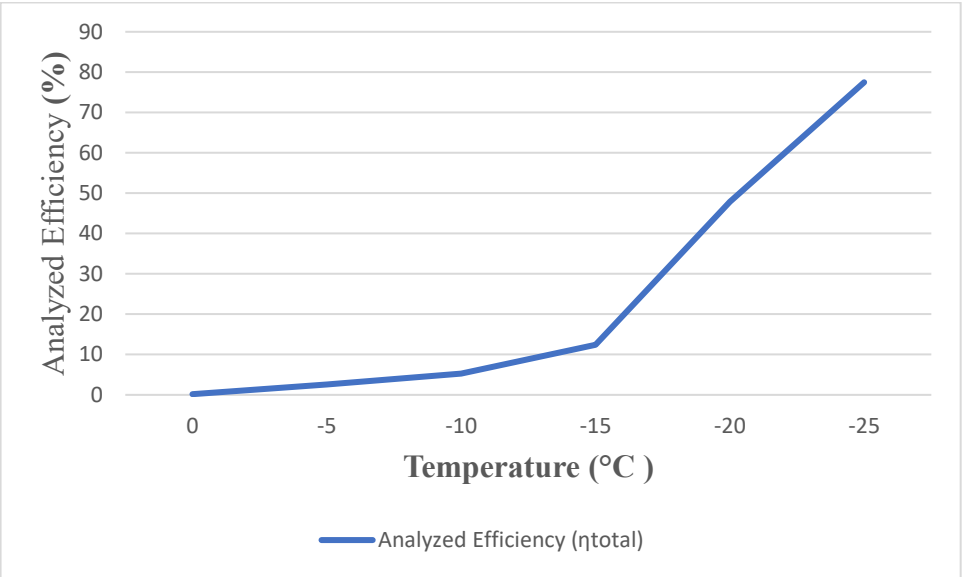

Figure 9.4 Analyzed Efficiency

Source: Author

10 Conclusion

This project deals with study of the influence of intake air temperature on the efficiency of the SR-30 microturbine learning model. Also process a correlation analysis of the device's efficiency on the intake air temperature.

Calculation of measured values shows that for the intake air temperature 5.48 °*C* have higher overall device efficiency it is about 6.35 % and thermodynamic efficiency for the higher temperature measurement values are low because of inner thermodynamic efficiency. It shows that running a turbine with low temperature intake air it leads to attain higher device efficiency because when the higher mass of air flowing through the turbine then the turbine efficiency will also increase.

The measured and evaluated data of SR-30 microturbine was processed for correlation analysis in mat lab. This correlation analysis process helps us to change the variety of intake air temperature and other parameters. Thus, this method leads us to increase the overall device efficiency by 77.48 % at the temperature of -25 °*C*. this project also deals with to improve the efficiency of the turbine, the air temperature was increased by using air heater which is connected in front of air inlet side of the turbine. The SR-30 microturbine performance characteristics were calculated for a set of variable intake air temperature.

11 References

1.Wartsila gas turbine. [Online] https://www.wartsila.com/energy/learn-more/technical-comparisons/gas-turbine-for-power-generation-introduction.

2. Characterizing the performance of the SR-30 turbojet engine. T. Witkowski, S. White, C. Ortiz Dueñas, P. Strykowski, T. Simon. 2003. Minnesota : s.n., 2003. American Society for Engineering Education.

3. Gas turbine efficiency Improvement by inlet air-cooling in sustainable energy system. Alavijeh, Omid zainali and Saeed karimi. 2015. 3, Assaluyeh, Bushehr : s.n., 2015, National Iranian Gas Company (NIGC), Vol. 8, pp. 18-24.

4. Zohuri, Bahman. 2015. Researchgate. [Online] 3 15, 2015. [Cited: 12 8, 2017.] https://www.researchgate.net/publication/300857212_Gas_Turbine_Working_Principles.

5. Araner. [Online] https://www.araner.com/blog/gas-turbine-theory/.

6. Wikipedia. [Online] https://en.wikipedia.org/wiki/Gas_turbine#cite_note-26.

7. Turbojet engine. [Online] https://www.turbinetechnologies.com/educational-lab-products/turbojet-engine-lab#4345-technical-papers.

8. Engine cutaway. [Online] https://www.turbinetechnologies.com/educational-lab-products/jet-engine-cutaway.

9. Matt Dietter, Kyle Lavoie, Kurtis Madden, Jonathan Sewell. 2016. Performance analysis and testing of the mini gas turbine. Boston : Wentworth institute of technology, 2016.

10. Tony Giampaolo, MSME, PE. 1939. Gas turbine handbook : principles and practices. Lilburn : The Fairmont Press, 1939.

11. Gas turbine. [Online] https://www.turbinetechnologies.com/Portals/0/pdfs/gas_turbine_tech_sheets/ME%204331.pdf.

12. Hush kit. [Online] https://www.turbinetechnologies.com/Portals/0/pdfs/specifications/HushKit%20Specs.pdf.

12 Acknowledgement

I am very grateful and lucky to work under my supervisor Ing. Petr Pavlik, Ph.D. who guided me through each step of my thesis work. His valuable guidance and technical support towards me are reason for my success in this thesis.

I sincerely express my gratitude to the department of power engineering for their supportive interactions and support in completion of this project.